Structural Investigation of Bond-Isomeric Hexakis (Thiocyanato-isothiocyanato) osmates (III) from Os L$_{III}$-Edge EXAFS

P. Rabe, G. Tolkiehn, A. Werner, and R. Haensel

Institut für Experimentalphysik, Universität Kiel

The extended x-ray absorption fine-structure (EXAFS) has been used to determine bond lengths and coordination numbers around the central Os-atom in bond-isomeric hexakis (thiocyanato-isothiocyanato) osmates (III) [Os(NCS)$_n$(SCN)$_{6-n}$]$^{3-}$, $n = 1, \ldots, 6$: The above assignment of the species with n-values is confirmed. The Os-N bond length decreases with increasing n while the Os-S bond length is the same in all compounds. The N-bonded ligands form an undistorted linear chain with the central Os-atom. The bond angles between the S-bonded ligands and Os-atoms are distorted by at least 10° around their average value ($\sim 105°$).

1. Introduction

The analysis of the extended x-ray absorption fine structure (EXAFS) which shows up above the absorption edges of atoms in molecules, liquids, and solids has developed to a reliable method for the determination of the short range order around the absorbing atom [1, 2, 3]. EXAFS is caused by an internal electron interference effect [4, 5]. The superposition of the outgoing photoelectron wave with parts of it backscattered from the neighbouring atoms results in a modulation of the matrixelement of the transition probability with the electron energy. Periodicity and amplitudes of EXAFS reflect the parameters of the local geometrical structure e.g. bond lengths and coordination numbers. Most of the investigations have been performed on EXAFS at K-edges. In this case only transitions to p-symmetric final states are possible. The analysis of EXAFS at K-edges of heavy elements is hindered by the increasing broadening of structures due to lifetime effects. For elements like Cu, Kr, or Ag the lifetime broadening amounts to 1.5 eV, 3 eV, and 7.5 eV, respectively, [6] which is tolerable for a structural analysis. For heavier elements this value increases rapidly. For Au e.g. the broadening of 54 eV [6] is of the same order as the periodicity of EXAFS so that the fine structure is effectively smeared out. Further experimental problems arise from the decrease of intensities even at high flux x-ray sources and decreasing reflectivities of crystals at high photon energies.

At L$_{III}$-edges the lifetime broadening is an order of magnitude smaller than for K-shells. Generally transitions to s- and d-symmetric final states contribute to the absorption coefficient in this case. However the probability μ_s for transitions to s-symmetric final-states is approximately a factor of 50 smaller than that to d-states (μ_d) [7, 8] so that those contributions can be neglected in all practical cases. The analysis of L$_{III}$-edge EXAFS can therefore be performed with techniques developed for K-shell EXAFS.

In this paper we report a structural analysis of the complexes [Os(NCS)$_n$(SCN)$_{6-n}$]$^{3-}$. Six of the seven possible complexes have been isolated by Preetz and Peters [9] by ion exchange chromatography. From the intensities of groups of lines in the IR and Raman spectra characteristic for the S- and N-bonded (SCN)-group the sequence has been attributed to $n = 1, 2, \ldots, 6$. Because of the complexity of this analysis independent criteria to confirm this assignment were desirable. Up to now it has not been successful to grow single crystals with good enough quality to determine the structure from x-ray diffraction experiments. Therefore we have analyzed the EXAFS beyond the L$_{III}$-edge of Os. From these spectra we evaluate the spherically averaged radial geometry around the absorbing Os atom. In the next section we briefly describe the experimental arrangement. In Sect. 3 we give a detailed analysis of the absorption spectra and evaluate coordination numbers for the first coordi-

nation spheres and the interatomic spacings between the central Os atom and the surrounding N, C, and S atoms.

2. Experimental Arrangement

The measurements have been performed at the Deutsches Elektronensynchrotron (DESY). The synchrotron-radiation is monochromatized with a channel-cut Si(220) crystal. In the energy range under consideration (10700 eV to 11 600 eV) the spectral resolution amounts to 3 eV. The intensities of the monochromatic radiation are monitored by Ar filled ionization chambers. The signals are digitized and stored in a computer. Details about the experimental setup are published in a forthcoming paper [10].

The compounds are available as salts of tetra-n-butylammonia (TBA) [9]. Each sample has been prepared from 55 mg of the Os-complex covered with 15 mg polyethylene on both sides under a pressure of 2 kbar in the form of foils of 32×4 mm^2 area. This technique yields polycrystalline samples of homogeneous thickness. The sample thickness has not been determined explicitly. To optimize the signal to noise ratio it has been chosen so that the transmission is 10% above the Os-L$_{III}$-edge. To reduce the influence of thermal motions of the atoms on the amplitudes of the EXAFS all samples have been cooled to liquid nitrogen temperature.

In addition to the compounds under investigation here, we have measured the absorption of dibromotetrapyridineosmium (II) [Os(py)$_4$Br$_2$]. In this complex the Os-N bond lengths are known from x-ray diffraction studies [11]. As shall be discussed later in detail, this material has been used as reference to determine the N backscattering amplitude and the phase shifts of the photoelectron wave for the Os-N atom pair.

3. Results and Discussion

For simplicity we shall label the isolated six samples with their index $n = 1, \ldots, 6$, all of which, except $n = 4$, have been investigated by EXAFS. As an example representative for all complexes we show the absorption spectrum of sample 6 in Figure 1. The contribution to the absorption coefficient due to transitions of weaker bond electrons has already been eliminated by a procedure described elsewhere [3]. This spectrum is charac-
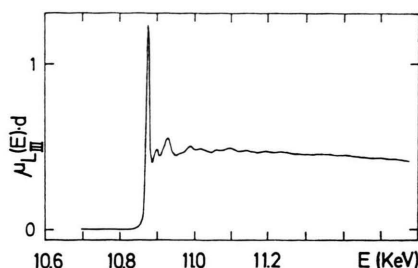

Fig. 1. Absorption spectrum of [Os(NCS)$_6$]$^{3-}$ at the Os L$_{III}$ edge. The background absorption due to excitations of weaker bound electrons has been removed.

terized by the L$_{III}$-edge at $E_{L_{III}} = 10868$ eV [12], and a white line right above the edge. This line is due to a high density of d-symmetric final states. It is omitted in the following data analysis. Beyond the line EXAFS shows up.

It is convenient to write the absorption coefficient in the following way

$$\mu(E) = \mu_0(E) \cdot (1 + \chi(E)) . \qquad (1)$$

Here E is the photon energy and μ_0 an atomic-like monotonous absorption coefficient which should be observed after removing all atoms surrounding the central Os atom.

Since mainly the transitions to d-symmetric states contribute to the transition probability for polycrystalline materials, the fine structure can be written in the following form (7):

$$\chi(k) = \frac{1}{k} \sum_i A_i(k) \sin(\psi_i(k)) \qquad (2)$$

$$\psi_i(k) = 2 k R_i + 2 \delta_d(k) + \arg(f_i(\pi, k)) , \qquad (3)$$

$$A_i(k) = |f_i(\pi, k)| (N_i/R_i^2) \cdot \exp(-2 \sigma_i^2 k^2) \exp(-2 R_i/\lambda) . \qquad (4)$$

Here, $f_i(\pi, k)$ is the complex scattering amplitude of the scattering atoms, N_i of which are located at an average distance R_i from the absorbing atom. The phase shift of the central atom is denoted by δ_d. A Gaussian pair distribution with mean square relative displacements σ_i^2 has been introduced to describe the displacement of the atoms around R_i due to thermal vibrations. The mean free path λ considers the damping of the photoelectron wave by inelastic scattering processes. The wavenumber k is calculated from the free electron dispersion

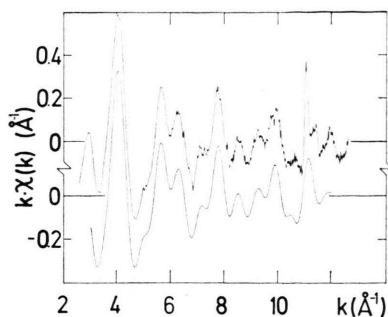$$k = \sqrt{\frac{2 m}{\hbar^2} (E - E_{L_{III}})} , \qquad (5)$$

Fig. 2. a) Experimental and b) Fourier filtered fine structure $k\chi(k)$ of $[Os(NCS)_6]^{3-}$.

where $E_{L_{III}}$ is the binding energy of electrons in the L_{III}-shell. The formal description of EXAFS by (2) is only valid for values $k \gtrsim 3 \text{ Å}^{-1}$, i.e. 50 eV above the edge. Below this value structures in μ are caused by variation of the density of states, by multiple excitations or by multiple scattering events which are not adequately described by (2).

Our experimental $k \cdot \chi(k)$ of sample 6 is shown in Figure 2a. The rapid decrease of the amplitudes of $k \cdot \chi(k)$ with increasing k is typical for scattering atoms with small atomic numbers, in this case N, C and S [13]. Figure 2b shows the same $k \cdot \chi(k)$ after applying a Fourier filtering which consists of a Fourier transform of $\chi(k)$ to real space and a subsequent inverse transform to k-space after truncating the data at $r = 6 \text{ Å}$. Only the presence of atoms at distances less than approximately 5 Å from the central atom leads to contributions to EXAFS. Therefore, both filtered and unfiltered spectra are identical apart from the statistical noise.

The Fourier filtered spectra of all measured samples are displayed in Fig. 3. A systematic change of the $\chi(k)$ is obvious: in going from $n = 6$ to $n = 1$, the amplitudes of $k \cdot \chi(k)$ at $k = 6.2 \text{ Å}^{-1}$ and 7.8 Å^{-1} decrease whereas at $k = 7.0 \text{ Å}^{-1}$ a structure grows up. Note the relatively large changes between $n = 3$ and $= 5$, which clearly confirms the missing of sample $n = 4$.

A preliminary conclusion about the type of scattering atoms can be drawn from the k-dependence of the amplitudes of $\chi(k)$. Compared to sample $n = 1$, where the envelope of $k \cdot \chi(k)$ has a maximum at $k \sim 5 \text{ Å}^{-1}$ we observe larger amplitudes at small k-values and a more rapid relative decrease of the amplitudes with increasing k for sample $n = 6$. This means that according to the k-dependence of $|f(\pi, k)|$ the dominant contribution to

$\chi(k)$ in $n = 6$ arises from the presence of N whereas the spectrum of $n = 1$ tells us that in this case the S atoms are dominating as nearest neighbors. Furthermore, in going from $n = 6$ to $n = 1$, the $k \cdot \chi(k)$ develop to the simpler form of a single oscillation. We conclude that in $n = 1$ the scatterers further apart from the central Os atom than the nearest neighbors are highly disordered.

So far we have discussed these spectra to demonstrate which conclusions about the local geometry in the vicinity of the absorbing atom can be drawn from the qualitative description of EXAFS. From the above discussion we have seen that the experimental $\chi(k)$ is a superposition of more than one oscillation with different frequencies in k-space. To separate these contributions we perform a Fourier transform to real space [2, 3]. Each term in (2) attributed to scatterers at R_i shows up as a peak in the magnitude of the Fourier transform $F(r)$. The amplitude of this peak is characterized by $A_i(k)$. The position is determined by the total phase $\psi_i(k)$ from which R_i can be evaluated. It should be noted that according to the k-dependent parts of $\delta_d(k)$ and $\arg(f_i(\pi, k))$ the positions of the peaks in $|F(r)|$ differ from the R_i by 0.2 to 0.5 Å.

The magnitude and the real part $\text{Re}(F(r))$ of the Fourier transform of the $k \cdot \chi(k)$ (Fig. 3) is shown in Figure 4. In all cases, the same range in k-space $(2.5 \text{ Å}^{-1} \leq k \leq 12.5 \text{ Å}^{-1})$ has been transformed. A Gaussian window function has been used to reduce truncation effects [3].

In the range $1.2 \text{ Å} \leq r \leq 2.5 \text{ Å}$ we observe two maxima at $r_1 = 1.67 \text{ Å}$ and $r_2 = 2.06 \text{ Å}$. According to the fact that the atomic radius of sulphur is approximately 0.4 Å larger than that of nitrogen we attribute the first peak at r_1 to the N scatterers and the second peak to the S scatterers. As expected, the amplitude of the peak at r_1 decreases in going from $n = 6$ to $n = 1$, whereas the peak at r_2 shows the opposite trend. This corresponds to the successive conversion from N-bonded to S-bonded SCN-groups. Two additional peaks in $|F(r)|$ of sample $n = 6$ at $r = 2.68 \text{ Å}$ and $r = 4.44 \text{ Å}$ are attributed to the C and the S atoms, respectively. In going to $n < 6$ these peaks decrease and, as expected from the $\chi(k)$, the $|F(r)|$ of sample $n = 1$ is dominated by a single S peak. Beyond $r = 3 \text{ Å}$ only two tiny structures in $|F(r)|$ of sample $n = 1$ are observed at 3.4 Å and 3.9 Å. Similar structures also show up in all the other $|F(r)|$ and are therefore attributed

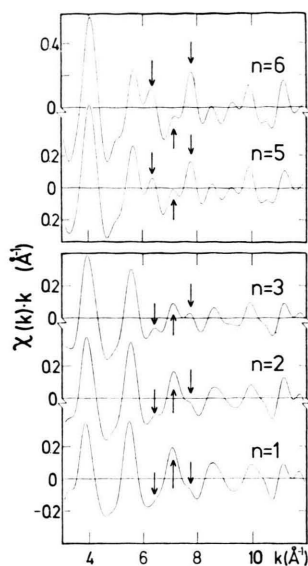Fig. 3. Fourier filtered $k\chi(k)$ of the measured $[Os(NCS)_n(SCN)_{6-n}]^{3-}$ complexes.

Fig. 4. Magnitude $|F(r)|$ and real parts Re $(F(r))$ of the Fourier transform over the range $2.5\ \text{Å}^{-1} \leq k \leq 12.5\ \text{Å}^{-1}$ using a Gaussian window calculated from the $k\chi(k)$ shown in Figure 3.

to spurious effects due to the data handling. The fact that the presence of C and N atoms in the thiocyanate complex yields no significant contribution to $\chi(k)$ can be explained with strong distortions of the Os-SCN bond angles. This leads to a certain spread of the Os-C and Os-N spacings and therefore to a destructive interference in $\chi(k)$ [14, 15]. Assuming an average bond angle of 105° we must conclude that in the complex $n = 1$ the bond angles for the thiocyanate ligands vary by at least 10°.

A linear arrangement of the Os-NCS in sample $n = 6$ can be deduced from an anomalous scattering phase of the Os-C and the Os-S pairs. For the S shell in $n = 6$, Re$(F(r))$ and $|F(r)|$ show a maximum at the same point ($r = 4.4$ Å). This means an additional phaseshift of approximately π compared to the S-scatterers in sample 1 where Re$(F(r))$ shows a minimum at the maximum value of $|F(r)|$. The same holds for the C shell in sample 6. According to the similar electronic structure of the atomic core of N and C, the phases of these scatterers differ only insignificantly. On comparing the first two shells for $n = 6$ in Fig. 4, an additional phase shift between these scatterers is observed. This behavior is typical for the case where a scatterer is shadowed by an other atom, i.e. where the central atom and two scatterers form a linear chain. Because of the strong peaking of the scattering amplitude in forward direction significant contributions to $\chi(k)$
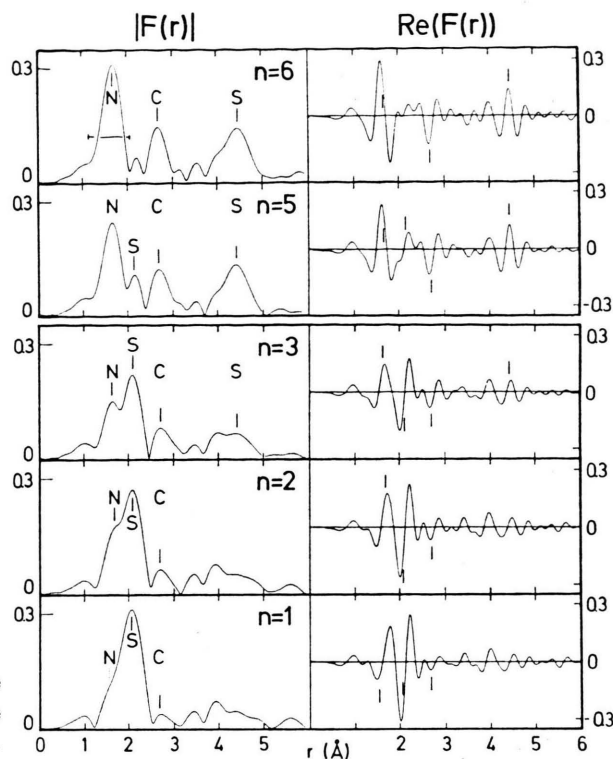
due to multiple scattering events are expected. A similar phase shift difference of π has been observed for the fourth neighbors in metallic Cu [2, 3], which together with the absorbing atom and its nearest neighbor form a linear chain.

The easiest way to extract absolute coordination numbers seems to be a direct comparison of the peaks in $|F(r)|$. According to Eq. (4) these amplitudes are directly proportional to N_i. This simple analysis leads to inconsistencies which are demonstrated in the following for the first N and S scatterers at $r = 1.67$ Å and $r = 2.06$ Å, respectively. The average difference Δ_S and Δ_N of the peak heights A_S and A_N between neighboring samples ($\Delta n = 1$) should correspond to a change of the coordination number by $\Delta N_i = 1$. The ratio A_N/Δ_N and A_S/Δ_S should then yield the coordination numbers of the N and S shell respectively. The results of this analysis shown in Table 1 predict seven in contrast to the maximum six bonds. The A_N/Δ_N values confirm the assignment of Preetz and

Table 1. Amplitudes A_N and A_S in arbitrary units of peaks in $|F(r)|$ (Fig. 4) attributed to the first N and S scatterers. $\Delta_N = 21.3$ and $\Delta_S = 19.9$ are the average alteration of A_N and A_S with $\Delta n = 1$. The analysis yields the incorrect result of seven Os bonds.

n	A_N	A_S	$N_N = A_N/\Delta_N$	$N_S = A_S/\Delta_S$	$N_N + N_S$
6	125.0	26.5	5.87	1.33	7.20
5	100.0	44.5	4.69	2.24	6.93
3	61.0	88.4	2.86	4.45	7.21
2		107.0		5.38	
1		126.0		6.33	

Fig. 5. Magnitude $|F(r)|$ and real part Re $(F(r))$ of $k\chi(k)$ of $[Os(NCS)_6]^{3-}$ calculated from the experimental $k\chi(k)$ spectrum (solid line) and from a two shell (N and C) model (dotted line) using calculated amplitude functions and scattering phases (8).

Peters [9], whereas the A_S/Δ_S predict an assignment altered by $\Delta n = -1$. The reasons for this inconsistency are to be found in the mutual interactions of the two peaks and influences of the C peak on the amplitudes of the first peak. Especially, the structure at 2.2 Å in $|F(r)|$ of sample 6 where in $|F(r)|$ of the other samples the S peak grows up is due to a constructive interference between N and C peak and has nothing to do with an S scatterer. To demonstrate this we have performed a Fourier transform of a model $\chi(k)$. This $\chi(k)$ has been calculated from Eq. (2) using theoretical back-scattering amplitudes and phase shifts [8] for the Os absorber and the scatterer N and C. For the C scatterer, an additional phase shift of π has been added to $\psi(k)$. The bondlengths and a scaling factor for the amplitudes $A_i(k)$ have been adjusted to give a best fit with the experimental data. In the resulting $|F(r)|$ (Fig. 5) a structure shows up at $r = 2.2$ Å similar to that observed in the $|F(r)|$ calculated from the measured $\chi(k)$. The remaining differences in the $F(r)$ are certainly due to the assumptions made in this model calculation, especially the assumption of a constant phase introduced by the multiple scattering. Nevertheless, this comparison shows that the peak at $r = 2.2$ Å in $|F(r)|$ is not caused by an S scatterer and we reach the conclusion that sample $n = 6$ has six N bonded SCN^- ligands in agreement with the proposed assignment of Preetz and Peters [9].

A first step to a more reliable way for the evaluation of coordination numbers and bond lengths is an inverse Fourier transform over a limited range in $F(r)$ [3] as indicated by a bar in Figure 4. First, we analyse the $\chi(k)$ of sample 6. If the assignment is correct, the result is a single term of Eq. (2) from which $A(k)$ and $\psi(k)$ for this shell
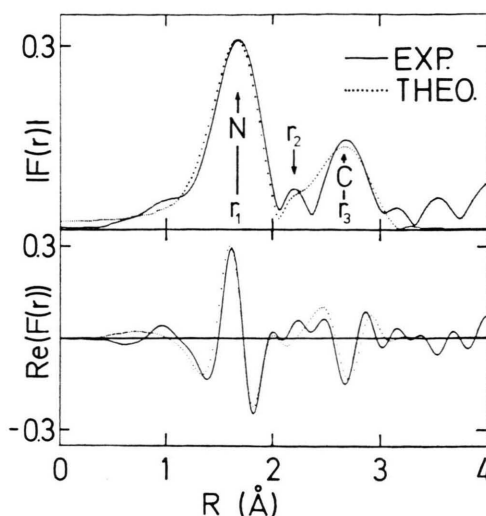
can be calculated. The bond length is then calculated from [3]

$$R(k) = (\psi(k) - \varphi(k))/(2k) . \tag{7}$$

Here, $\varphi(k)$ is the sum of the absorber and scatterer phase. The phase shift $\varphi(k)$ is known to be transferable i.e. we can either use calculated $\delta_d(k)$ and $\arg(f(\pi, k))$ or determine $\varphi(k)$ from $\chi(k)$ of a reference compound with the same absorber and scatterer pair and with known bond length. The k-scales of the $\psi(k)$ and $\varphi(k)$ may differ. To compensate those differences we have varied $E_{L_{III}}$ in Eq. (5) in a way so as to obtain a constant $R(k)$ over the whole k range. Using an experimental phase $\varphi_E(k)$ evaluated from an Os-L_{III} absorption spectrum of $[Os(py)_4Br_2]$ where the Os-N bond length has been determined by x-ray diffraction ($R = 2.09 \pm 0.04$ Å) [11] we obtain $R_E = 2.07 \pm 0.045$ Å (Figure 6a). The error is the sum of the uncertainty for R of the reference material (0.04 Å) and the deviation of $R(k)$ from a horizontal straight line (0.005 Å). In Fig. 6b we have included $R_T(k)$ obtained with a theoretical phase $\varphi_T(k)$ [8] which has been approximated by a polynomial of second degree in k. From this analysis we get $R_T = 2.13 \pm 0.04$ Å which is significantly larger than R_E. The error of 0.04 Å is the sum of the difference between polynomial and tabulated value (0.01 Å), the
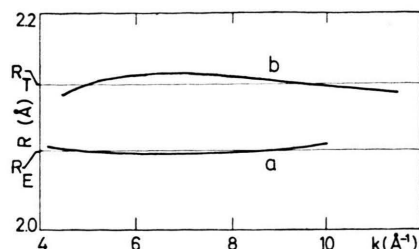
Fig. 6. Determination of Os-N bond lengths using Eq. (6) and $\varphi(k)$ a) determined from an absorption spectrum of $[Os(py)_4Br_2]$ and b) taken from [8].

deviation of $R_T(k)$ from a constant (0.01 Å) and a typical error of 0.02 Å for $\varphi_T/(2k)$ [3].

In the same way using the calculated phase shift [8] we determined the bond lengths for the next nearest C neighbors in $n = 6$. To account for the shadowing of the C atoms by the N atoms a constant phase of π has been added to $\varphi_T(k)$. The result for the Os-C distance is $R_T = 3.19 \pm 0.05$ Å.

The coordination number for sample 6 is evaluated from

$$\ln(A_6(k)/A_B(k)) = -2(\sigma_6^2 - \sigma_B^2)k^2$$
$$+ \ln\left(\frac{N_6}{N_B} \cdot \frac{R_B^2}{R_6^2}\right) \qquad (8)$$

where the index B denotes the reference compound. In this analysis we have assumed equal values for λ in both samples. A plot of the result of Eq. (8) versus k^2 is shown in Figure 7. Using R_B and N_B of the reference material and the values of R_6 determined above, we get $N_6 = 5.72 \pm 0.4$ atoms in agreement with the results of Preetz and Peters [9]. Additionally the slope of the straight line in Fig. 7 tells us that the mean square relative displacements σ^2 of the Os-N pair in $[Os(NCS)_6]^{3-}$ is smaller by an amount of $\Delta\sigma^2 = 0.0025$ Å^2 in comparison to σ_B^2 of the same atom pair in $[Os(py)_4Br_2]$.
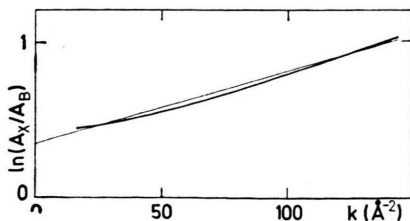

Fig. 7. Determination of the N coordination number of $[Os(NCS)_6]^{3-}$ from $\ln(A(k)/A_B(k))$ [Eq. (8)] at $k = 0$ where $A(k)$ and $A_B(k)$ are the amplitude functions of the nearest neighbor N scatterer in $[Os(NCS)_6]^{3-}$ and $[Os(py)_4Br_2]$, respectively. The slope of the straight line yields $\Delta\sigma^2 = 0.0025$ Å^2.
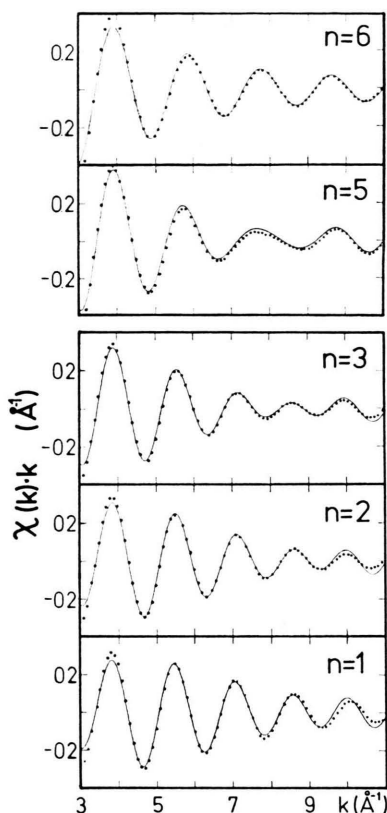

Fig. 8. Contribution to the fine structures $k\chi(k)$ caused by the first N and S shells calculated from an inverse Fourier transform over the range $1.2\ \text{Å} \leq r \leq 2.5\ \text{Å}$ (solid lines). The dotted lines are the $k\chi(k)$ fitted to the experimental fine structures using the parameterized Equation (9).

For the samples $n < 6$ an inverse Fourier transform over the range $1.2\ \text{Å} \leq k \leq 2.5\ \text{Å}$ yields a filtered EXAFS spectrum which is described by a sum over two terms in Equation (2). The results of this transform are shown in Fig. 8 as solid lines. To isolate each term and to calculate the bond lengths and coordination numbers of the individual N and S shells we have analysed these data by a fitting procedure. The fine structure has been represented by

$$k \cdot \chi(k) = \sum_{i=1}^{2} \frac{p_{1i}}{1 + b_{2i}^2(k - b_{3i})^2} \qquad (9)$$
$$\cdot e^{-p_{2i}k^2} \sin(p_{3i}k + a_{2i}k^2 + a_{3i})$$

with

$$p_{1i} = b_{1i}(N_i/R_i^2)e^{-2R_i/\lambda}, \qquad (10)$$

$$p_{2i} = 2\sigma_i^2, \qquad (11)$$

$$p_{3i} = 2R_i + a_{1i}. \qquad (12)$$

The parameters a_{ji} and b_{ji} $(j = 1, 2, 3)$ are known from tabularized and parameterized amplitude functions of N and S and phase shifts [8, 16] of the pairs Os-N and Os-S so that in total six free parameters have been used to fit the experimental data. The best fits have been included in Fig. 8 as dotted lines. In detail we obtain the following results:

a) Bond Lengths

Together with the R-values of sample 6 determined above we have summarized the bond lengths of all compounds in Table 2. The Os-N bond length of sample 6 obtained from the fit is identical with the value R_T obtained above which shows the reliability of the fitting technique. It is interesting to note that the Os-N bond length increases with decreasing number of N bonded ligands whereas the Os-S bond length of $R = 2.50$ Å remains unchanged within an experimental uncertainty of less than 0.01 Å. This means that the S-bonded ligands squeeze out the N-bonded ligands. Furthermore we have considered that two different Os-N bonds might exist in sample 6. A fit with two shells results in a similar bond length for both components thus ruling out this possibility.

To confirm the increasing Os-N bond length with decreasing n we have investigated the beating introduced by a superposition of two contributions to Eq. (2) with different k-dependence of the $\psi(k)$ [17]. The amplitudes $\tilde{A}_n(k)$ of the finestructures shown in Fig. 8 ($n < 6$) normalized to the amplitude $A_6(k)$ of the fine structure for $n = 6$ have been plotted in Figure 9. The minima in $\tilde{A}_n(k)/A_6(k)$ marked by arrows move to higher k-values with decreasing n. These minima show up at

$$k_{\min} = (m\pi - \Delta\varphi)/(2\Delta R) \quad (m = 1, 3, 5, \ldots). \quad (13)$$

Here $\Delta\varphi$ is the difference of the phases φ of the S- and the N-shell. The difference in bondlengths of the two shells is denoted by ΔR. In the region of interest $\Delta\varphi$ amounts to 3.6 rad [8]. Using this value and the experimental $k_{\min}$ we obtain the ΔR values as listed in Table 2. We observe an excellent agreement between the $\Delta R_{(B)}$ determined from the beating and the $\Delta R_{(T)}$ calculated from the fitted R values. For sample $n = 1$ the more reliable value for ΔR is the value extracted from the beating.

Using the bondlengths of the first N-shell in sample 6 (2.13 Å) determined above and the peak-position in $|F(r)|$ ($r = 1.67$ Å) yields the shift
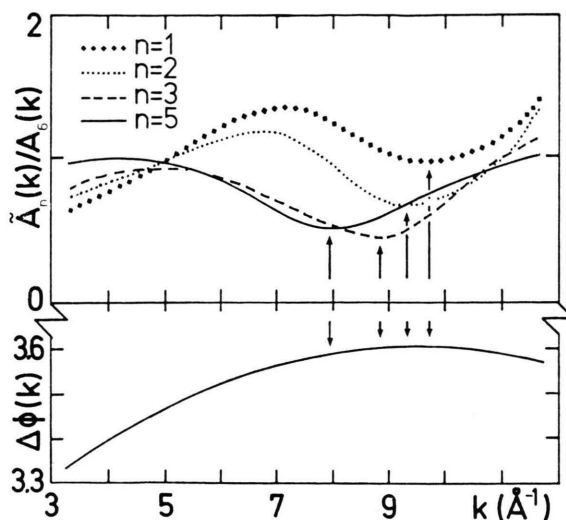

Fig. 9. a) Ratio of the amplitudes of $\chi(k)$ of the fine structure for $n < 6$ shown in Fig. 8 to the amplitude of $\chi(k)$ for $n = 6$. From the minima as indicated by arrows ΔR between N and S shell has been calculated. b) Difference of phase shift $\Delta\varphi(k)$ between the $\varphi(k)$ of the pairs Os–S and Os–N taken from [8].

Table 2. Bond lengths in Å between Os and the nearest N and S neighbors. $R_{N(R)}$ and $R_{N(T)}$ determined from eq. 6 with phase $\varphi(k)$ extracted from an absorption spectrum of $[Os(py)_4Br]^{2-}$ and theoretical phase shifts (8) respectively; $R_{N(F)}$ and $R_{S(F)}$ determined from a fit of a two shell $\chi(k)$ calculated from an inverse Fourier transform over a limited range in $F(r)$ (see Fig. 4) using calculated scattering amplitudes and phase shifts; $\Delta R_{(F)} = R_{S(F)} - R_{N(F)}$; $\Delta R_{(B)}$ difference of R_S and R_N obtained from the beat frequency.

n	$R_{N(R)}$	$R_{N(T)}$	$R_{N(F)}$	$R_{S(F)}$	$\Delta R_{(A)}$	$\Delta R_{(B)}$
6	2.07	2.13	2.13			
5			2.13	2.50	0.37	0.37
3			2.16	2.50	0.34	0.33
2			2.21	2.50	0.29	0.31
1			(2.26)	2.51	(0.25)	0.30

$\alpha = 0.46$ Å which is caused by the k-dependent parts of $\varphi(k)$ and which is characteristic for the Os-N pair. Assuming that α for Os-C has the same value according to the similar electronic structure of N and C we can simply determine the Os-C distance from the position of the C-peak in $|F(r)|$. The result of $R = 3.16$ Å is close to the value determined above using theoretical phases (Table 3). The same analysis for the S-shell in sample 6 yields $R = 4.89$ Å with α taken from the bondlength of the first S-shell in sample 1 and the corresponding peak position (Fig. 4).

Table 3. Os–C and Os–S distance in $n = 6$. R–α is the peak position in $|F(r)|$ and R the true bondlength. For the C scatterer, the α of the first N peak in Fig. 4 ($n = 6$), for the S scatterer the α of the first S peak in Fig. 4 ($n = 1$) has been used. R_c is the Os-C distance determined from Eq. (6) using calculated phase shifts of Ref. [8] and an additional constant phase of π due to multiple scattering. All values in Å units.

	N ($n = 6$)	C ($n = 6$)	S ($n = 1$)	S ($n = 6$)
$R - \alpha$	1.67	2.70	2.06	4.44
α	0.46	0.46	0.45	0.45
R	2.13	3.16	2.15	4.89
R_c		3.19		

b) Coordination Number

The fitted p_{1i} values ($i =$ N or S) are directly proportional to the coordination numbers N_i. In Fig. 10 we have plotted these values versus n on the basis of the assignment of Preetz and Peters [9]. The linear regressions through the data points shown as solid lines in Fig. 10 have been calculated from

$$p_{1S}(6 - n) = A_S n + B_S ,$$
$$p_{1N}(n) \quad = A_N n + B_N . \tag{14}$$

If the assumed assignment is correct, the intersection with the vertical axis at $n = 0$ should take
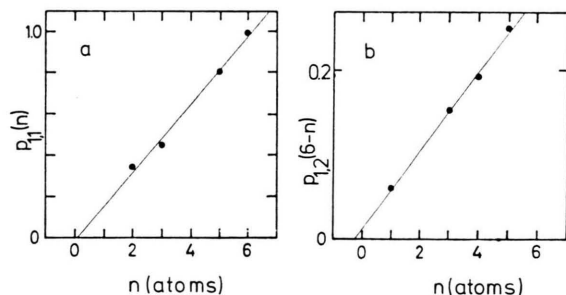

Fig. 10. Plot of the fitted parameter p_{1i} (Eq. (9)) versus coordination number n: a) N-shell ($i = 1$); b) S-shell ($i = 2$).

the value of $B = 0$. A change of the assignment by $\Delta n = \pm 1$ would lead to $B = \pm A$. From the linear regressions we obtain

$$A_N = 0.165, \qquad B_N = -0.013 ,$$
$$A_S = 0.047, \qquad B_S = \quad 0.012 .$$

Both B values are significantly smaller than the A values, which again confirms that the sequence $n = 1, \ldots, 6$ has been isolated. The error in this determination of relative coordination numbers amounts to 0.13 atoms in our investigations.

If reference compounds of known geometry, as discussed in this paper, are not available, absolute coordination numbers can be determined using calculated backscattering amplitudes. From a linear regression

$$p_{1S}(6 - n) = D_S n ,$$
$$p_{1N}(n) \quad = D_N n \tag{15}$$

we obtain $D_S = 0.0507$ and $D_N = 0.1620$. Using $R = 2.13$ Å and the calculated $b_{1N} = 1.600$ [16] for nitrogen, we obtain from (10) a mean free path $\lambda = 5.48$ Å. Together with this value of λ, a bond length $R = 2.50$ Å and the calculated $b_{1S} = 0.779$ [16] for the S-shell, we determine a theoretical $D_S = 0.0500$. The excellent agreement between the calculated and the experimental value of D_S demonstrates the reliability of the concept of transferability of amplitude functions.

[1] F. W. Lytle, D. E. Sayers, and E. A. Stern, Phys. Rev. B 11, 4825 (1975).
[2] E. A. Stern, D. E. Sayers, and F. W. Lytle, Phys. Rev. B 11, 4836 (1975).
[3] G. Martens, P. Rabe, N. Schwentner, and A. Werner, Phys. Rev. B 17, 1481 (1978).
[4] E. A. Stern, Phys. Rev. B 10, 3027 (1974).
[5] P. A. Lee and J. B. Pendry, Phys. Rev. B 11, 2795 (1975).
[6] L. G. Parratt, Rev. Mod. Phys. 31, 616 (1959).
[7] P. Rabe, G. Tolkiehn, and A. Werner, J. Phys. B 12, 899 (1979).
[8] B.-K. Teo and P. A. Lee, J. Amer. Chem. Soc. 101, 2815 (1979).
[9] W. Preetz and G. Peters, Z. Naturforsch. 34b, 1243 (1979).

[10] P. Rabe, G. Tolkiehn, and A. Werner, submitted to Nucl. Instr. & Meth.
[11] H.-L. Keller, private communication.
[12] J. A. Bearden and A. F. Burr, Rev. Mod. Phys. 39, 125 (1967).
[13] P. A. Lee and G. Beni, Phys. Rev. B 15, 2862 (1977).
[14] D. E. Sayers, E. A. Stern, and F. W. Lytle, Phys. Rev. Lett. 27, 1204 (1971).
[15] P. Rabe, G. Tolkiehn, and A. Werner, J. Phys. C 12, L 545 (1979).
[16] B.-K. Teo, P. A. Lee, A. L. Simons, P. Eisenberger, and B. M. Kincaid, J. Amer. Chem. Soc. 99, 3854 (1977).
[17] G. Martens, P. Rabe, N. Schwentner, and A. Werner, Phys. Rev. Lett. 39, 1411 (1977).